The Meteoritical Society

Meteoritics & Planetary Science 1–15 (2010)
doi: 10.1111/j.1945-5100.2010.001096.x

The midinfrared transmission spectra of multiple stones from the Almahata sitta meteorite

Scott A. SANDFORD[1*], Stefanie N. MILAM[1,2†], Michel NUEVO[1], Peter JENNISKENS[2], and Muawia H. SHADDAD[3]

[1]NASA Ames Research Center, MS 245-6, Moffett Field, California 94035, USA
[2]SETI Institute, Carl Sagan Center, 515 North Whisman Road, Mountain View, California 94043, USA
[3]Department of Physics and Astronomy, University of Khartoum, P.O. Box 321, Khartoum 11115, Sudan
[†]Present address: NASA Goddard Space Flight Center, Code 691, Greenbelt, Maryland 20771, USA
[*]Corresponding author. E-mail: Scott.A.Sandford@nasa.gov

(Received 06 November 2009; revision accepted 16 June 2010)

Abstract–On October 7, 2008 the asteroid 2008 TC3 entered the Earth's atmosphere, exploded at 37 km altitude, and created a strewn field of stones, the Almahata Sitta meteorite, in Sudan. A preliminary analysis of one of these stones (#7) showed it to be a unique polymict ureilite (Jenniskens et al. 2009). Here we report 39 midinfrared (mid-IR) (4000–450 cm^{-1}; 2.5–22.2 μm) transmission spectra taken from 26 different stones collected from the strewn field. The ureilite spectra show a number of absorption bands including a complex feature centered near 1000 cm^{-1} (10 μm) due to Si-O stretching vibrations. The profiles of the silicate features fall along a mixing line with endmembers represented by Mg-rich olivines and pyroxenes, and no evidence is seen for the presence of phyllosilicates. The relative abundances of olivine and pyroxene show substantial variation from sample to sample and sometimes differ between multiple samples taken from the same stone. Analysis of a mass normalized coaddition of all our ureilite spectra yields an olivine:pyroxene ratio of 74:26, a value that falls in the middle of the range inferred from the infrared spectra of other ureilites. Both the predominance of olivine and the variable olivine-to-pyroxene ratio are consistent with the known composition and heterogeneity of other ureilites. Variations in the colors of the samples and the intensities of the silicate feature relative to the mass of the samples indicate a significant contribution from additional materials having no strong absorption bands, most likely graphitized carbon, diamonds, and/or metals.

INTRODUCTION

The small (approximately 4 m in diameter) asteroid 2008 TC3 (spectral class F) was discovered by the automated Catalina Sky Survey telescope on October 6, 2008 at 06:39 UTC (Kowalski et al. 2008). The asteroid impacted the Earth's atmosphere over the Nubian Desert of northern Sudan (Chesley et al. 2008; Yeomans 2008) only 20 h after discovery. The fall of the body was observed both by satellites (Brown 2008; Borovicka and Charvat 2009) and by eyewitnesses on the ground (Jenniskens et al. 2009). Based on some 570 astrometric positions of the asteroid's approach path, the probable location of the strewn field of possible surviving material was calculated and a dedicated search in this area was carried out by enthusiastic students and staff of the University of Khartoum. All the samples discussed in this paper were found during field campaigns (December 6–8 and 26–30, 2008) which recovered a total of 52 fragments of the Almahata Sitta (''Station 6'') meteorite having a total mass of about 3.5 kg. Masses range from a few mg to 283 g. Stones were found spread for 29 km along the approach path of the asteroid in a manner expected for debris from 2008 TC3 (Jenniskens et al. 2009).

Nearly all recovered meteorites showed abundant fusion crust and a broken face with no corresponding pieces nearby. One of these stones (#7) was fragmented

M A P S | 1096-1257 | B | Dispatch: 26.8.10 | Journal: MAPS | CE: Vijay
Journal Name | Manuscript No. | Author Received: | No. of pages: 15 | PE: Karpagavalli

and pieces distributed for analysis by a multitude of techniques, including oxygen isotope analysis, bulk chemistry, mineralogy, as well as visible and infrared (IR) spectroscopy. The combined results of these studies were reported in Jenniskens et al. (2009) and showed that this stone was an anomalous polymict ureilite. Mineral compositions of Almahata Sitta #7 were not found to be anomalous, but its textures were, including only rare zoning of olivine, larger size carbonaceous aggregates, fine-grained texture, high metal content, and high porosity with possible vapor-phase mineral growth of olivine. Measured porosities of Almahata Sitta stones fall in the 25–37% range, equal to the high porosities of primitive carbonaceous chondrite meteorites.

Ureilites were initially thought to derive from S-class asteroids (Gaffey et al. 1993) in the Tholen taxonomic classification of asteroid reflectance spectra (Tholen 1989). However, measurements of the albedo of Almahata Sitta #7 yielded a low value of 0.046 ± 0.005 in the V-band for the darker samples. The reflectance spectra of both 2008 TC3 and Almahata Sitta meteorite #7 are most similar to F- or B-class asteroids (for "flat" and "blue-sloped," respectively) (Jenniskens et al. 2009). B-class asteroids tend to show a 3 μm OH-stretch vibration band due to hydrated silicates. In our earlier work, the infrared spectra of Almahata Sitta #7 showed only a very weak 3 μm OH-stretch band that was likely due to minor adsorbed telluric water. In addition, the spectra of Almahata Sitta #7 also showed no substructure in the Si-O stretching band near 10 μm that is diagnostic of phyllosilicates. Thus, we concluded that 2008 TC3 was an F-class asteroid and the Almahata Sitta meteorite establishes a link between F-class asteroids and the ureilites (Jenniskens et al. 2009).

A striking aspect of Almahata Sitta was the wide range of textures and albedos for individual meteorites. Many meteorites show a range of grain sizes and are very dark in appearance, while others had a fine-grained texture and much lighter gray color. Despite this diversity, they all ended up inside an approximately 28 m^3 volume of a parent asteroid. An important question is how these materials differ on a microscopic scale and how they relate to each other.

Ureilites are carbon-bearing ultramafic rocks with an enigmatic history. We will make no attempt here to summarize the detailed nature of this class of meteorites or the many models proposed for their genesis. For more details about ureilites, the reader is referred to Goodrich (1992), Goodrich et al. (2004), Middlefehldt et al. (1998), Downes et al. (2008), and the many references within these works, as well as other articles in this issue. Here we will only summarize key points associated with major mineralogy that impacts the infrared spectra of these meteorites.

Polymict ureilites, of which Almahata Sitta is one (Jenniskens et al. 2009), provide considerable insights in the nature of the ureilite parent body that cannot be obtained from monomict samples (Goodrich et al. 2004; Downes et al. 2008). While electron microprobe analyses of olivine and pyroxene clasts in polymict ureilites show a statistically identical range of compositions to that found in unbrecciated ureilites, polymict ureilites contain a variety of clasts with indigenous lithologies that are not seen in monomict samples. They also contain multiple types of nonureilitic impactor and impact-derived materials. The combined information obtained from the polymict ureilites suggests that the ureilites derive from a common parent asteroid, with the polymict ureilites representing near-surface regolith materials (Goodrich et al. 2004; Downes et al. 2008).

Ureilites typically consist of millimeter-sized aggregates of magnesian olivine and subordinate clinopyroxene. The pyroxenes are most commonly pigeonite, but admixtures of augite and other pyroxenes are also seen. The olivine abundance is typically about twice that of the pyroxene (Sandford 1993), although there are a few reported examples where their abundances are approximately equal. The olivines and pyroxenes exhibit heterogeneity in Mg content between meteorites, with forsterite contents ranging from Fo_{74} to Fo_{97}, with most falling between Fo_{74} and Fo_{85} (Takeda 1991; Goodrich et al. 2004; Downes et al. 2008). Coexisting pyroxenes typically show similar Mg abundances. Subordinate to the olivines and minerals are dark interstitial material (<10%) consisting principally of graphite, diamond, lonsdaleite, Ni-poor metal, and troilite (Vdovykin 1970; Berkley et al. 1976, 1978, 1980). Fine grained graphite is the most common carbon polymorph in these meteorites, although large mm-sized euhedral crystals have been seen in a few ureilites.

Midinfrared spectra of meteorites can provide useful information on the composition of many of their dominant minerals. For an excellent compilation of discussions on infrared spectroscopy of minerals, see Farmer (1974). Midinfrared laboratory transmission and reflection spectra of many different meteorite classes are already available (i.e., Sandford 1984, 1993; Miyamoto 1987; Salisbury et al. 1991), but relatively little attention has been paid to ureilites. The largest compilation of spectra can be found in Sandford (1993), which describes the mid-IR spectra of seven different ureilites. Not surprisingly, the mid-IR spectra of ureilites are dominated by the spectral features of olivines and pyroxenes, the two dominant minerals in these meteorites. Other phases have relatively little impact on the spectra either because of their low abundance or, as in the case of graphite and diamond, because they have

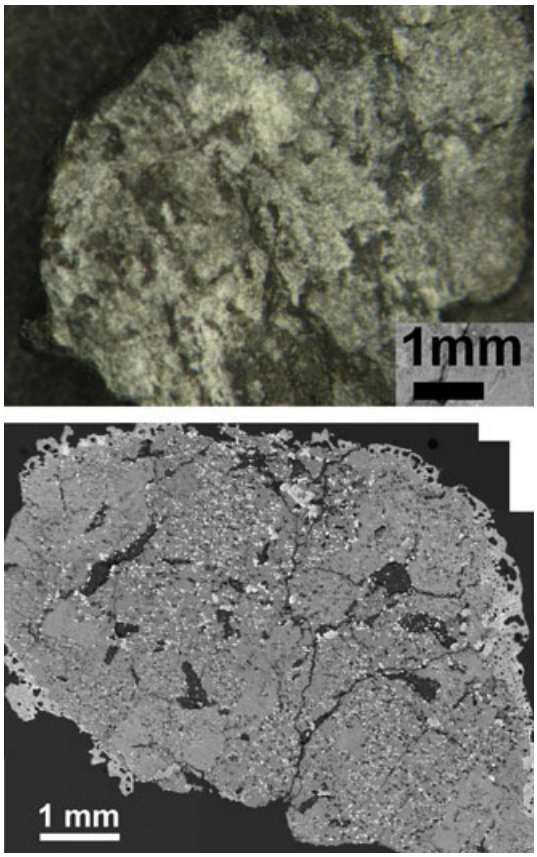

Fig. 1. (Top) An image of the surface of an exposed interior portion of Almahata Sitta #7. This stone was very friable and showed distinct dark and light phases. (Bottom) Back-scattered electron image of a cross section of the same sample of Almahata Sitta #7 showing both compact and friable lithologies. Dark regions are C-rich areas and pores, bright regions are kamacite and Fe-Ni-Cr sulfides, and gray regions are dominated by low Ca pyroxenes (En72–98) and olivines (Fo84–92), and some pigeonite (images courtesy of M. Zolensky).

infrared absorption features that are intrinsically very weak.

The infrared spectra briefly described in Jenniskens et al. (2009) were taken from samples of Almahata Sitta #7 (Fig. 1). This material showed distinct dark and light phases and a small sample was taken from each. Milligram-sized samples of each phase were ground in KBr and pressed into pellets. The spectra (Fig. 2) show Si-O stretching features characteristic of a mixture of olivine and pyroxene with olivine being the more abundant mineral, consistent with previous IR spectra taken from ureilites (Sandford 1993). However, only limited material was available and it was not clear whether these two spectra of Almahata Sitta #7 were (1) characteristic of the Almahata Sitta #7 stone as a whole and (2) similar to the spectra of other Almahata Sitta stones. In this paper we present 39 mid-IR

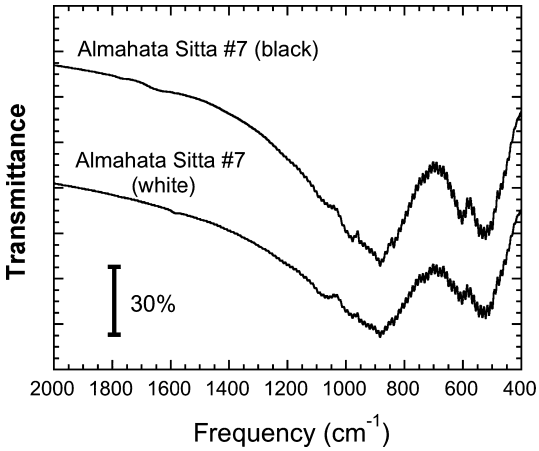

Fig. 2. The infrared transmission spectra from 2000 to 400 cm^{-1} (5–25 μm) of (top) a course grained fraction of Almahata Sitta #7 having a black visual appearance, and (bottom) a finer grained fraction having a white visual appearance. Despite the large contrast in visual appearance, both samples show Si-O stretching features characteristic of olivine-pyroxene mixtures with olivine being more abundant, consistent with the spectra of other ureilites (see Sandford 1993). Both spectra were obtained from mg-sized meteorites samples diluted and ground in KBr (sample:KBr = 1:100) and pressed into 100 mg pellets.

(4000–450 cm^{-1}; 2.5–22.2 μm) transmission spectra taken from 26 different stones collected from the Almahata Sitta strewn field in order to better quantify the variation in composition of different stones and to better assess the spectrum of the meteorite as a whole.

In the following section (Sample Selection, Preparation, and Measurement) we discuss the selection and preparation of the meteorite samples, and the experimental techniques used to obtain their spectra. The results of these studies are shown in Results and a discussion of the implications of these results is presented in Discussion.

SAMPLE SELECTION, PREPARATION, AND MEASUREMENT

All the samples examined in this study were taken from small fragments broken off during normal handling of the meteorites. Because the total available samples of most of the stone examined were very small, and because these materials were to be examined by numerous analytical techniques (see the other papers in this special issue), only limited samples were available for this study. Typical total sample sizes obtained were in the 5–10 mg range, although a few were smaller due to lack of available material. A summary of the samples we studied is given in Table 1. In many cases a spectrum was measured from only a single sample from a particular stone. In other cases we were able to obtain

Table 1. Summary of Almahata Sitta samples studied.

Sample	Mass of stone (g)	Mass of sample (mg)	Mass of KBr (mg)	Mass of pellet (mg)	Pellet color[a]	Number of scans[b]	Dominant mineral type
4#1	14.592	2.90	289	99.8	7	100	Olivine
4#2	14.592	5.21	530	99.8	7	200	Olivine
7B[c]	1.5200	2.50	261	101.5	4.5	100	Olivine
7W[c]	1.5200	1.35	139	100.8	7	200	Olivine
15#1	75.536	1.86	188	100.6	4	50	Olivine
15#2[d]	75.536	3.16	321	100.6	3	200	Pyroxene
19	4.8590	2.31	233	102.8	5	150	Olivine
24	92.760	2.34	234	100.2	5.5	100	Olivine
25[e]	221.95	2.05	206	100.5	4	100	Mixed
27	283.84	2.28	234	101.8	6	120	Olivine
28	32.131	3.09	312	101.6	4.5	150	Olivine
29	55.417	4.71	470	100.9	6	80	Mixed
31	88.796	2.13	215	100.3	3	60	Pyroxene
32A	130.40	3.44	347	100.4	5	120	Pyroxene
32B#1	130.40	2.91	296	100.4	3	100	Olivine
32B#2[f]	130.40	2.78	280	100.7	4.5	200	Olivine
34	32.985	2.09	208	100.6	6	180	Olivine
36A#1	57.880	3.16	316	100.8	5	80	Olivine
36A#2	57.880	2.61	265	100.4	5	280	Mixed
36B	–	3.99	399	101.0	4.5	100	Mixed
37	155.08	2.77	282	101.5	5	100	Olivine
39A#1	5.6610	3.55	357	102.1	6.5	200	Olivine
39A#2	5.6610	3.46	349	100.3	7	280	Olivine
39A#3	5.6610	3.93	391	100.8	6	280	Olivine
42A	72.092	3.20	323	101.4	5	220	Olivine
42B[g]	72.092	2.08	209	100.3	4	250	Pyroxene
44	2.2910	4.90	491	101.9	4.5	100	Mixed
46	162.15	1.50	150	99.5	5	200	Mixed
47	79.112	3.50	351	101.4	5	160	Olivine
48	152.11	3.30	330	100.2	5	110	Olivine
49	4.7100	3.45	345	99.8	5.5	200	Olivine
50	25.312	4.84	485	100.4	4.5	60	Olivine
51#1	20.197	3.65	366	100.2	2	100	Pyroxene
51#2	20.197	2.34	235	100.5	4	220	Pyroxene
51#3	20.197	3.87	389	101.2	1.5	150	Pyroxene
51#4	20.197	4.03	404	100.7	3	100	Pyroxene
52	16.895	3.88	391	101.6	3	80	Mixed
53	95.342	2.72	272	101.1	5	80	Olivine
54	121.22	3.90	393	100.1	5	80	Mixed
Fibers[h]	–	–	–	–	–	400	–
Density Sand	–	4.13	416	101.4	Orange	50	–

[a]Numbers refer to the grayscale below.
[b]All ratios done to 300 scans of background unless otherwise noted.
[c]The IR spectra discussed in Jenniskens et al. (2009) were taken from this stone.
[d]Unique pyroxene spectrum (see text).
[e]This stone has been determined to be an H5 ordinary chondrite by Zolensky et al. (2010, this issue).
[f]Sample selected to include only green crystalline grains; chosen as the olivine spectral endmember.
[g]Sample chosen as the pyroxene spectral endmember.
[h]Fibers taken from sample can 39B; fibers were not put in KBr pellets but transmission spectra were instead taken directly from the fibers suspended over an aperture and ratioed to a 500 scan background spectrum taken from the blank aperture.

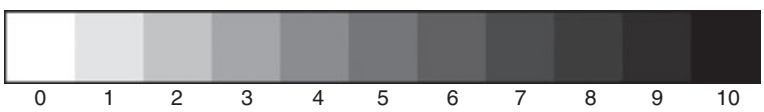

enough material from a stone to make multiple samples and measurements.

During the course of our studies it was determined that stone #25 is not a ureilite, but is instead an H5 ordinary chondrite (Zolensky et al. 2010, this issue). Whether this stone represents an unrelated find or represents a xenolith from the Almahata Sitta parent body is not presently clear. Given the large number of meteorites found during the search for fragments of 2008 TC3, and that they were found in a dry environment conducive for the survival and discovery of meteorites, it would not be surprising if one or more of the collected stones was unrelated to the 2008 TC3 event. Conversely, polymict ureilites have been seen to contain xenoliths of other classes of meteorites including R, CI1, and E chondrite materials (see Bischoff et al. 2006 and references therein). It has been estimated that 20–30% (by mass) of the recovered meteorites in the strewn field are not ureilites, but it has been suggested that some of these stones belonged to 2008 TC3 because the distribution of their ground locations is similar to the ureilites (Shaddad et al. 2010, this issue). Independently, Bischoff et al. (2010) and Horstmann and Bischoff (2010) have also suggested that numerous nonureilite stones found within the Almahata Sitta strewn field were part of the 2008 TC3 parent body. Our spectra of material from stone #25 are presented along with the spectra of the other stones, but its distinction as an ordinary chondrite is noted where relevant.

Sample Selection

We were able to select samples from 26 different stones recovered in the first two field searches. Material from these stones was stored in small aluminum sample cans with glass windows in their lids. Careful examination of the contents of these containers showed that many of them contained one or more contaminants (1) A modest number of cans contained very thin, clear glass shards. These were clearly contaminants that had broken off the edges of the glass in the lids of the cans. These materials were distinctly different from the meteorite samples and could be easily avoided. (2) Many of the cans contain a scattering of orange-tinted, rounded grains that look identical to the sand grains used earlier to make density measurements of the individual stones (Shaddad et al. 2010, this issue). Because these grains were typically quite large and had a distinctive orangish color, they could be easily avoided during sample selection. We took a sample of these grains and measured their spectrum for comparison with the meteorite samples as a means of assessing possible spectral contamination (see Results). (3) Additionally, a few of the cans contained small fibers. These fibers are sometimes seen individually, but they often were in ''knots'' or ''clumps'' that, in some cases, look like tiny seeds. A number of these were removed and their spectrum obtained for comparison with the meteorite samples as a means of assessing possible spectral contamination. Again, these materials were easily distinguishable from the meteorites samples and were avoided. (4) Finally, fragments with fusion crust, which were easily identifiable under the microscope, were avoided when selecting our samples.

Typical materials in the meteorites consisted of a dark, porous/friable matrix, often with visible embedded crystals. The crystals often looked colorless or greenish, but sometimes had a reddish tinge, and were generally submillimeter in size, although larger crystals were occasionally seen. The samples from most stones looked qualitatively similar and wherever possible an attempt was made to select and use samples that were representative of the material available from each stone. Several samples are worthy of additional comment, however.

The material from stone #7 was very friable and contained a mixture of very fine grained light colored materials and larger, stronger clumps of darker materials. The darker clumps looked similar to the material common to the other stones. Two samples were taken from stone #7, one dominated by the friable light colored material (7W) and one dominated by the darker clumps (7B). [Note that stone #7 is the original stone examined from Almahata Sitta by Jenniskens et al. (2009).] The available material from stone #32 also contained an atypically large proportion of finer grained materials as well as large green mineral crystals that could be easily separated from their surrounding matrix. In this case we were able to prepare two separate samples, one dominated by the finer grained material (32B#1) and one containing only the large crystals (32B#2). Samples 42A and 42B were similarly selected: 42A consisted of material representative of the overall available material, while 42B was selected to be dominated by the large green crystals present in this stone.

The first number in our sample names (see Table 1) always refers to the stone from which the sample was obtained. If this number is followed by a letter, this signifies samples taken from separate sample cans or samples preselected for a specific phase. If multiple, unbiased samples were made from a given specimen, they are designated with a final number.

It is worth noting that the olivine-pigeonite aggregates in ureilites are typically 0.1–2.0 mm in diameter with an average of about 1 mm (see Berkley 1986), but domains as large as 7 mm have been reported. While the material in Almahata Sitta #7 is

anomalously fine-grained, this may not be true for all the stones from which samples were obtained. In addition, many samples contained larger, individual mineral grains within the matrix. Thus, there exists the possibility that some of the samples described above could be dominated by local heterogeneities and thus fail to be representative of the original stone as a whole. Where possible, we have prepared and measured multiple samples from the same stone (see Table 1, denoted by subsample numbers #1, #2, etc.) to help assess the extent of this issue.

Sample Preparation

The majority of the samples were prepared using the standard KBr pellet techniques described in Sandford (1984, 1993). In most cases, every attempt was made to pick relatively uniform aliquots from each of the available meteorite samples. In a few cases, as indicated in Table 1, an attempt was made to select a sample that was dominated by a particular phase. For example, sample 32B#2 consisted solely of green crystals selected from the larger 32B stone. Typically, samples of a few mg were mixed with 100 times their mass of KBr (Sigma-Aldrich, 99 + %, FT-IR grade) and then ground mechanically for 2 min in an all-steel ball mill. Approximately 100 mg of the resulting powder was then compress in a 1.5 cm diameter die at 1.1×10^8 Pa for 1 min to make a thin pellet suitable for IR transmission measurements. The resulting variability in sample density and column depth between the various meteorite samples is expected to be on the order of 1% (Table 1). While the column density of the material in the KBr pellets was very uniform, the pellet colors were not. Individual pellet colors ranged from near-white to near-black. The grayscale color of the pellets was determined by comparing each pellet to a grayscale "key" (see Table 1), with an error of ±1 on this scale.

The contaminant fibers were not expected to grind well and they were measured directly by suspending them over a 2 mm diameter aperture placed in the focal point of the spectrometer sample chamber. In this configuration many of the IR photons missed the sample entirely, resulting in lowered absorption band contrast. It is also possible that some of the stronger absorption bands could show saturated absorption profiles. Nonetheless, the resulting spectra were of sufficient quality to demonstrate that the fiber produced spectra very different from the meteorite samples.

Measurement of Infrared Spectra

The spectra were taken using a Bio-Rad Excalibur Fourier transform infrared spectrometer equipped with a Globar source, a KBr beamsplitter, and a liquid nitrogen-cooled mercury-cadmium-telluride detector. Spectral coverage extended from 7000 to 450 cm^{-1} (1.43–22.2 μm) and spectra were measured at a resolution of 1 cm^{-1}, which is more than adequate to resolve mid-IR mineral bands. During measurement, the KBr pellets were mounted over a 4 mm wide aperture placed in the focal point of the spectrometer's sample chamber. Single beam spectra of the samples were ratioed against a background spectrum obtained earlier through the same aperture. With this system it was generally possible to obtain spectra with signal-to-noise ratios of approximately 0.2% in a modest number of scans. The number of scans used was therefore usually determined by selecting a scan time that provided good cancelation of atmospheric H_2O and CO_2 bands by the background spectrum (see Table 1). No additional corrections for telluric gases were made to the spectra.

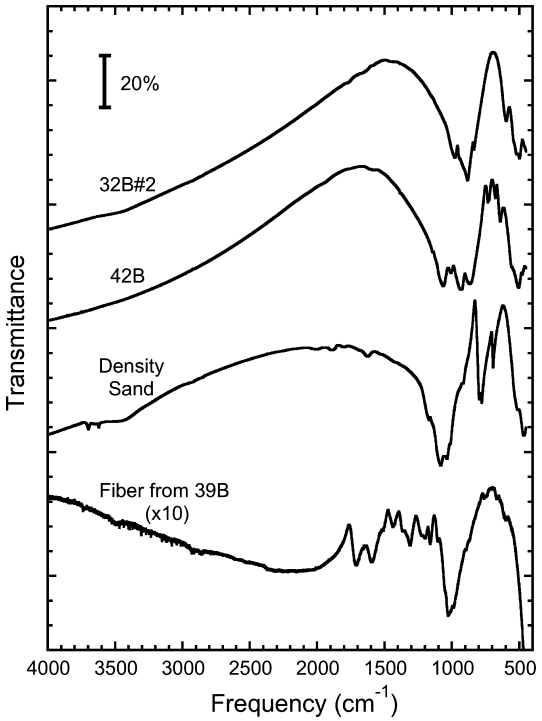

Fig. 3. The 4000–450 cm^{-1} (2.5–22.2 μm) infrared transmission spectra of Almahata Sitta endmember samples 32B#2 (olivine) and 42B (pyroxene), a sample of the contaminant "sand" used to make previous density measurements of the meteorite, and contaminant fibers found in the sample container for stone #39.

RESULTS

Figure 3 shows the 4000–450 cm^{-1} (2.5–22.2 μm) infrared transmission spectra of Almahata Sitta samples 32B#2 and 42B, a sample of the contaminant "sand"

used to make previous density measurements of the meteorite, and contaminant fibers found in the sample container for stone #39. The spectra of samples 32B#2 and 42B are shown since they represent "endmembers" of the distribution of spectra produced by the meteoritic samples. Their significance will be discussed in more detail later. It is clear that the spectra of the two contaminants are very different from the meteorite samples (Fig. 3). No evidence of any of the specific spectral features characteristic of these contaminants is seen in any of the meteorite spectra we obtained. We are therefore confident that these are not of concern and will not be further addressed in this paper.

The spectra of samples 32B#2 and 42B are typical of all Almahata Sitta spectra in that they do not show any absorption features of significance at frequencies above 2000 cm^{-1} (below 5 μm). Broad, very weak features are seen to varying extents in the meteorite spectra, but these are largely, if not entirely, due to small amounts of telluric H_2O adsorbed onto the KBr and/or meteorite grains. Since the remaining absorption features of interest are all associated with minerals and fall to lower frequencies, we will only show spectra in the 2000–450 cm^{-1} (5.0–22.2 μm) range in subsequent figures. This range spans the various silicate mineral Si-O stretching modes between 1200 and 700 cm^{-1} (8.3–14.3 μm) and covers some of the longer wavelength silicate O-Si-O bending modes that fall beyond 700 cm^{-1}.

As will be shown, all but one of the meteorite spectra can be described by a simple mixing of two spectral endmembers dominated by olivine and pyroxene, respectively. The top two spectra in Fig. 4 shows the 2000–450 cm^{-1} (5–22.2 μm) infrared transmission spectra of sample 32B#2 (the olivine endmember) and a Guadalupe ultramafic xenolithic (GUX) olivine standard. Their similarities are readily apparent feature for feature. The third spectrum of sample 42B represents the pyroxene-dominated endmember of the observed distribution. The fourth spectrum is of sample 15#2, which showed a unique pyroxene-like spectrum different from that of the other Almahata Sitta samples dominated by pyroxene. The bottom two spectra were obtained from pigeonite standards B18247 and 117671 graciously provided by the Smithsonian Institution's Department of Mineral Sciences.

Figures 5–9 show the 2000–450 cm^{-1} (5–22.2 μm) spectra obtained from all the meteorite samples studied. For convenience, the spectra have been organized into figures showing spectra dominated by olivines (Figs. 5–7), pyroxenes (Fig. 8), and mixtures of the two (Fig. 9). It should be noted however, that these figures do not represent distinct "classes" of material; with the exception of sample 15#2, all the spectra fall on various points along a mixing line between the olivine and pyroxene endmembers. The predominance of the minerals olivine and pyroxene is broadly consistent with mineralogical studies of samples from numerous Almahata Sitta stones, which are observed to be dominated by three main lithologies (1) a pyroxene-dominated, very porous, highly reduced lithology, (2) a pyroxene-dominated compact lithology, and (3) an olivine-dominated compact lithology (Zolensky et al. 2010, this issue).

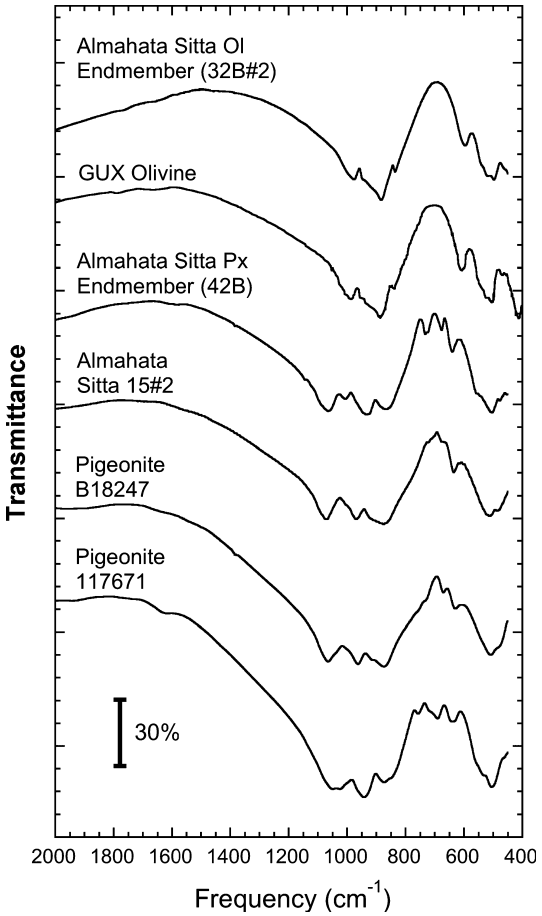

Fig. 4. From top to bottom: the 2000–450 cm^{-1} (5.0–22.2 μm) infrared transmission spectra of sample 32B#2, a Guadalupe ultramafic xenolith (GUX) olivine standard, samples 42B and 15#2, and pigeonite standards B18247 and 117671. The first and third spectra represent the olivine and pyroxene endmembers, respectively, of the spectral distribution obtained from all the meteorite spectra. The spectrum of sample 15#2 is unique among our Almahata Sitta samples (see text). The pigeonite standards were kindly provided by the Smithsonian Institution Department of Mineral Sciences.

The spectra dominated by olivine show subfeatures near 980, 885, 835, 600, and 500 cm^{-1} (10.2, 11.3, 12.0, 16.7, and 20.0 μm, respectively), with the band near 885 cm^{-1} being most prominent (Table 2, Figs. 5–7). The observed band positions and relative depths are very characteristic of olivines. The spectra dominated by

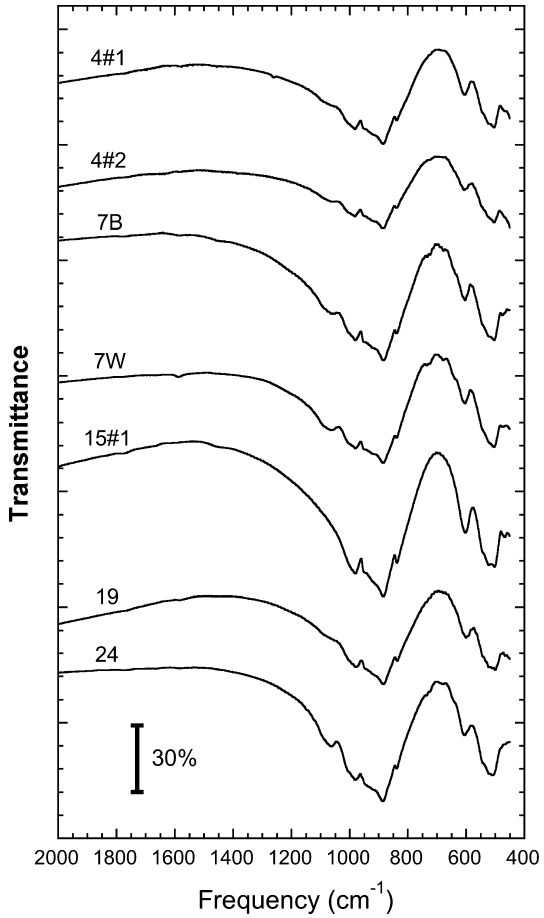

Fig. 5. The 2000–450 cm^{-1} (5.0–22.2 μm) infrared transmission spectra of seven samples dominated by olivine taken from five stones of the Almahata Sitta meteorite.

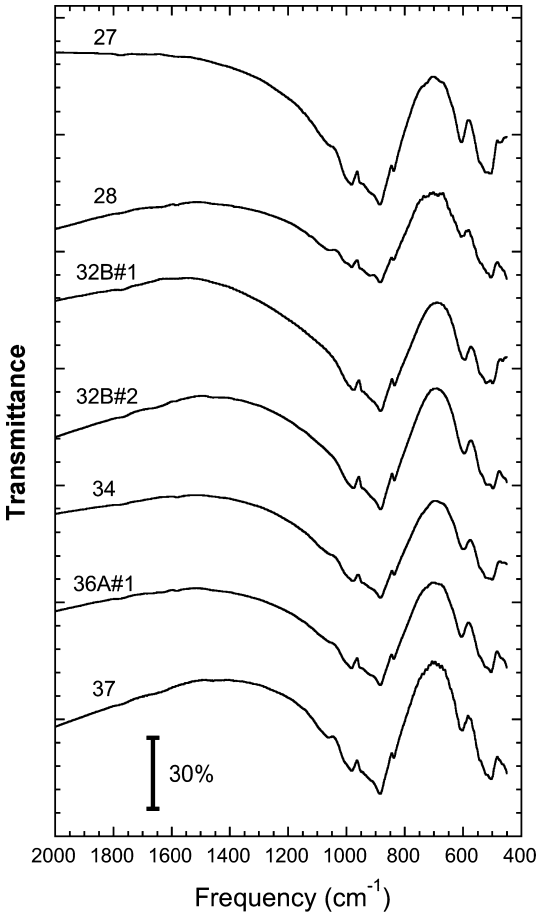

Fig. 6. The 2000–450 cm^{-1} (5.0–22.2 μm) infrared transmission spectra of seven samples dominated by olivine taken from six stones of the Almahata Sitta meteorite. The spectrum of sample 32B#2 was used as the olivine spectral endmember for the determination of olivine-to-pyroxene ratios in all the samples.

pyroxenes (Table 2, Fig. 8) typically show subfeatures that fall near 1065, 1010, 935, 870, 730, 675, 640, and 510 cm^{-1} (9.39, 9.90, 10.7, 11.5, 13.7, 14.8, 15.6, and 19.6 μm, respectively). Of these, the first four produce the dominant "10 μm" band and have roughly equal strengths. The unique spectrum of sample 15#2 is also consistent with a pyroxene, but shows a somewhat simpler spectrum. It shows subfeatures near 1070, 970, 875, 635, and 515 cm^{-1} (9.35, 10.3, 11.4, 15.7, and 19.4 μm, respectively). Of these, the first three produce the dominant "10 μm" band and have roughly equal strengths. These band positions and their assignments for the major spectral features of the olivine and pyroxene endmembers are summarized in Table 2.

The KBr pellets showed a systematic tendency to be darker as the olivine/pyroxene ratio increases. The grayscale average (Table 1) for pellets producing spectra dominated by olivine (Figs. 5–7) was 5.4 ± 1.1, while pellets dominated by pyroxene (Fig. 8) had a much lighter grayscale average of 3.2 ± 1.1. Samples with spectra of more equal mixtures of olivine and pyroxene (Fig. 9) fall in the middle of this range with a grayscale average of 4.6 ± 0.9. Darker pellets also showed lower infrared continuum throughput outside the silicate feature, with the continuum transmission decreasing by approximately 5% per unit increase in grayscale value.

It is interesting to note that there is a variety of ureilite (the "Hughes group") in which the dominant mineralogy is pyroxene and there is almost no carbon (Downes et al. 2008). If the darkening of the pellets is due to increased carbon content, the systematic tendency for our pellets to be darker with increasing olivine/pyroxene ratio could be consistent with the admixture of "Hughes group"-like materials in the 2008 TC3 parent body.

There is also a weak tendency for decreased overall silicate band strengths (measured by band area) as the pellets become darker.

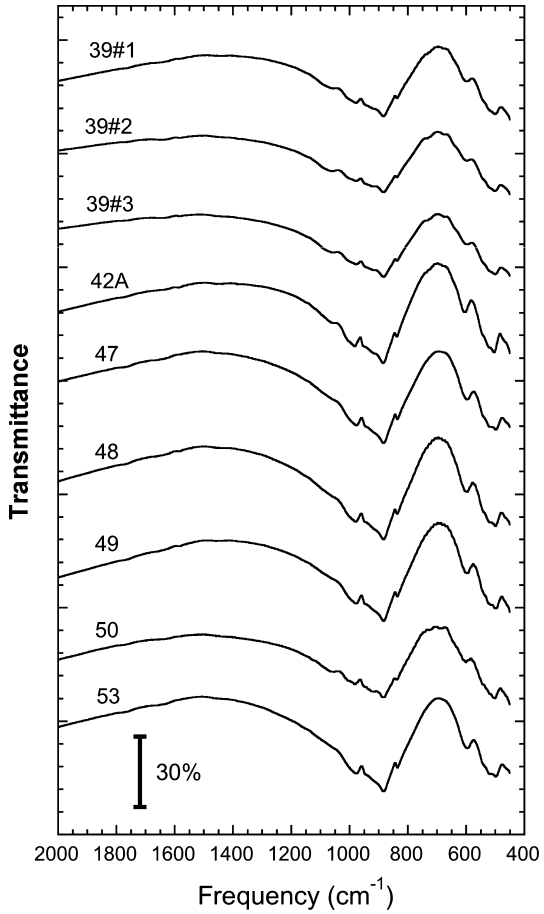

Fig. 7. The 2000–450 cm^{-1} (5.0–22.2 μm) infrared transmission spectra of nine samples dominated by olivine taken from seven stones of the Almahata Sitta meteorite.

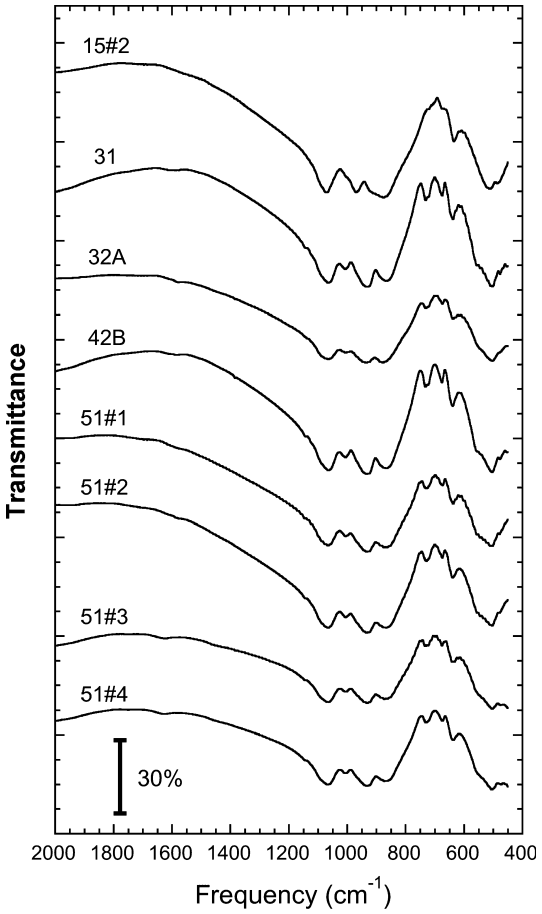

Fig. 8. The 2000–450 cm^{-1} (5.0–22.2 μm) infrared transmission spectra of eight samples dominated by pyroxene taken from five stones of the Almahata Sitta meteorite. The spectrum of sample 42B was used as the pyroxene spectral endmember for the determination of olivine-to-pyroxene ratios in all the samples. Sample 15#2 yielded a pyroxene spectrum different from all the other samples examined in this work.

DISCUSSION

The Meteoritic Silicate Features—Mineralogy

The broad absorption features centered near 1000 and 500 cm^{-1} (10 and 20 μm) are due to Si-O stretching and O-Si-O bending vibrations, respectively. The detailed profiles of these bands depend on the crystalline structure of the silicates and can therefore be used to identify the major mineral components present (cf. Farmer 1974; Sandford 1984; Hamilton 2000). Comparison with data from the terrestrial olivine and pyroxene standards (Fig. 4) clearly indicates that the spectra of Almahata Sitta samples are dominated by these two minerals, with their relative proportions varying from sample to sample. This is consistent with the principle mineralogy established for numerous Almahata Sitta samples using other techniques (Zolensky et al. 2010, this issue).

The overlapping of the various olivine and pyroxene bands complicates the use of the spectra to derive the olivine-to-pyroxene ratios in the samples. However, several of the stronger subfeatures of olivine and pyroxene can be used as indicators of the presence of each of these minerals. In particular, an absorption feature near 1065 cm^{-1} is indicative of pyroxenes and a band near 885 cm^{-1} is characteristic of olivines. Sandford (1993) used ratios of these two features to derive approximate olivine-to-pyroxene ratios from a group of seven ureilites and was able to obtain values accurate to approximately 10%.

Here we estimate the proportions of olivines and pyroxenes in the Almahata Sitta samples using a similar, but computationally more sophisticated approach. After examination of all the data, the spectra of samples 32B#2 and 42B were selected as representatives of the pure olivine and pyroxene endmembers of the observed spectral distribution, respectively (see Fig. 4). The spectra of these two

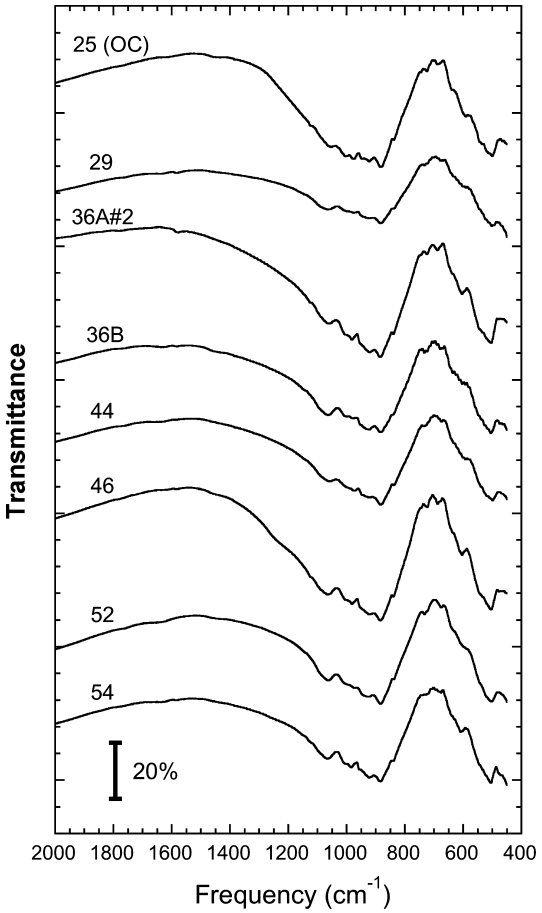

Fig. 9. The 2000–450 cm^{-1} (5.0–22.2 μm) infrared transmission spectra of eight samples containing appreciable amounts of both olivine and pyroxene taken from eight stones of the Almahata Sitta meteorite. Sample 25 has been determined to be an H5 ordinary chondrite (Zolensky et al. 2010, this issue).

Table 2. Tentative mineral identifications to the various absorption bands in the spectra of Almahata Sitta.

Band position[a] (cm^{-1})	Band position (μm)	Assignment[b]
1065	9.39	Pyroxene (s)
1010	9.90	Pyroxene (s)
985	10.3	Mg-rich olivine (m)
935	10.7	Pyroxene (s)
885	11.3	Mg-rich olivine (s)
835	11.9	Mg-rich olivine (w)
730	13.7	Pyroxene (w)
675	14.8	Pyroxene (w)
640	15.6	Pyroxene (w)
600	16.7	Mg-rich olivine (m, s)
510	19.6	Pyroxene (s)
500	20.0	Mg-rich olivine (s)

[a]Typical position observed rounded to the nearest 5 cm^{-1}.
[b]Absorptions whose intrinsic relative strengths are weak, medium, and strong are designated as (w), (m), and (s), respectively.

samples were used as "standards" to determine the relative abundances of olivine and pyroxene of all other meteoritic samples studied in this work.

Each of the infrared spectra, including the olivine and pyroxene endmembers, was first baseline corrected using spline interpolations (combination of polynomial functions) over the 2000–450 cm^{-1} region, and then rescaled so that the intensity of the peak of the olivine (approximately 885 cm^{-1}) or pyroxene (approximately 935 cm^{-1}) bands was renormalized to a value of 1. An IDL routine was then used to compare these modified spectra one by one to a suite of IR spectra built from normalized additions of the olivine and pyroxene endmember spectra of samples 32B#2 and 42B, respectively, using the equation:

$$\begin{aligned} f_{\text{test}}(i) &= g_{\text{oliv}}(i) f_{\text{oliv}} + g_{\text{pyr}}(i) f_{\text{pyr}} \\ &= g_{\text{oliv}}(i) f_{\text{oliv}} + (1 - g_{\text{oliv}}(i)) f_{\text{pyr}}, \end{aligned} \quad (1)$$

where $f_{\text{test}}(i)$ is the individual synthesized spectrum built from the addition of the standard olivine and pyroxene IR spectra f_{oliv} and f_{pyr}, respectively, weighted by the proportions of olivine ($g_{\text{oliv}}(i)$) and pyroxene ($g_{\text{pyr}}(i)$) in spectrum i, where $g_{\text{pyr}}(i) = 1 - g_{\text{oliv}}(i)$. Each normalized meteorite spectrum was then compared with all of the synthesized spectra and a $\chi^2(i)$ value was calculated using:

$$\chi^2(i) = 1/N \sum [f_{\text{sample}}(k) - f_{\text{test}}(k)]^2, \text{with } 1 \le k \le N, \quad (2)$$

where N is the total number of points k of the spectra in the range where the calculation was performed. The smallest value of χ^2 determined the synthesized spectrum, and therefore the proportions of olivine (g_{oliv}) and pyroxene (g_{pyr}), that provided the best fit to each sample spectrum.

Synthesized spectra were calculated using 0.001 increments of g_{oliv} and g_{pyr}. Thus, 1001 different spectra were compared with each sample spectrum. The entire process of comparing each normalized meteorite spectrum to all of the synthesized spectra was carried out twice—once over the 1498–700 cm^{-1} range that spans the nominal main olivine silicate feature, and once over the 1672–700 cm^{-1} range that spans the nominal main pyroxene silicate feature. The 700 cm^{-1} short wave number limit was chosen to avoid high χ^2 values caused by different slopes under the features in the 700–450 cm^{-1} range.

The normalized χ^2 values, as well as the best fit olivine and pyroxene proportions, were found to be very insensitive to whether we compared across the 1498–700 cm^{-1} (olivine) or 1672–700 cm^{-1} (pyroxene) ranges. Table 3 provides a summary of the relative proportions of olivine and pyroxene associated with the lowest χ^2 values when the wider 1672–700 cm^{-1}

Table 3. Summary of olivine-pyroxene composition analyses.

Sample	χ^2	% Olivine	% Pyroxene
4#1	0.420	93	7
4#2	1.045	88	12
7B	0.459	80	20
7W	1.038	80	20
15#1	0.358	93	7
15#2[a]	4.079	0	100
19	0.288	100	0
24	1.430	94	6
25[b]	3.142	46	54
27	1.296	78	22
28	0.527	81	19
29	0.206	56	44
31	0.184	7	93
32A	2.868	0	100
32B#1	0.261	88	12
32B#2[c]	0.000	100	0
34	0.216	91	9
36A#1	0.414	88	12
36A#2	0.631	64	36
36B	0.333	43	57
37	0.642	100	0
39A#1	0.337	98	2
39A#2	0.302	81	19
39A#3	0.342	87	13
42A	0.720	100	0
42B[d]	0.000	0	100
44	0.140	57	43
46	0.878	30	70
47	0.075	99	1
48	0.046	93	7
49	0.856	100	0
50	0.671	84	16
51#1	2.967	0	100
51#2	2.649	0	100
51#3	0.836	1	99
51#4	0.472	4	96
52	0.398	64	36
53	0.056	95	5
54	0.493	55	45
Mass weighted average (w/o stone 25)	0.314	74	26
Mass weighted average (all stones)	0.389	71	29

[a]Unique pyroxene spectrum (see text).
[b]This stone was determined to be an H5 ordinary chondrite by Zolensky et al. (2010, this issue).
[c]Olivine spectral endmember.
[d]Pyroxene spectral endmember.

(pyroxene) range was used. These values are expected to be accurate to better than 5%, with the chief uncertainty being associated with the possible presence of minor amounts of other infrared-absorbing materials. In this respect, it is interesting to note that the unique pyroxene spectrum of sample 15#2 is identified by this algorithm as being 100% pyroxene, even though it differs from the chosen pyroxene endmember, although the fit has a larger χ^2 value than other pyroxene endmembers. The spectrum of Almahata Sitta #25, the H5 ordinary chondrite, shows a nearly even mix of olivine and pyroxene (Table 3).

Individual spectra fall essentially everywhere along the entire range from pure olivine to pure pyroxene. However, olivine is clearly more prevalent than pyroxene overall. An estimate of the "average" olivine to pyroxene ratio for Almahata Sitta can be derived by coadding all of the spectra normalized to the total masses of the individual stones from which their respective samples were obtained (Table 1). This was done in two steps. First, for those stones from which we were able to obtain the spectra of multiple samples, all the spectra were averaged to produce a single spectrum to represent each stone. Stones for which we only had one spectrum needed no averaging. We then coadded the representative spectra of the stones with the contribution of each spectrum weighted by the mass of its associated stone. This was done both for all the stones combined and for all the stones excluding sample 25. Figure 10 shows the spectrum that results when data from sample 25 are omitted. This represents our best estimate of the spectrum of the "bulk" Almahata Sitta parent body (assuming sample 25 is from an unrelated fall and not an H5 xenolith), compared to the spectral olivine and pyroxene endmembers. (It should be noted that we obtain essentially the same spectrum if all the data are coadded with no mass weighting and whether or not we include the spectrum from sample 25.)

The same process of determining relative proportions of olivine and pyroxene was applied to this averaged spectrum. The result for the ureilite samples (i.e., all our spectra except that of sample 25) was an olivine:pyroxene ratio of 74:26 with a χ^2 value of 0.314 (if the sample 25 OC spectrum is included the ratio is 71:29 with a χ^2 value of 0.389). Sandford (1993) used a similar but less sophisticated approach to estimate the olivine-to-pyroxene ratios (accurate to approximately 10%) from a group of seven ureilites and found olivine:pyroxene ratios that ranged from 45:55 to 95:5 with olivine dominating in most of the samples. The Almahata Sitta value falls very near the center of this range. For comparison, Takeda (1987) and Takeda et al. (1989) have reported values for olivine:pigeonite of 48:52 for Y74659, 85:10 for Y790981, 80:15 for ALHA77257, 65:26 for ALHA82106, and values ranging from 63:36.5 to 95:5 for META 78008. Modal pyroxene/(pyroxene + olivine) ratios summarized in Middlefehldt et al. (1998) range from 0 to approximately 0.9.

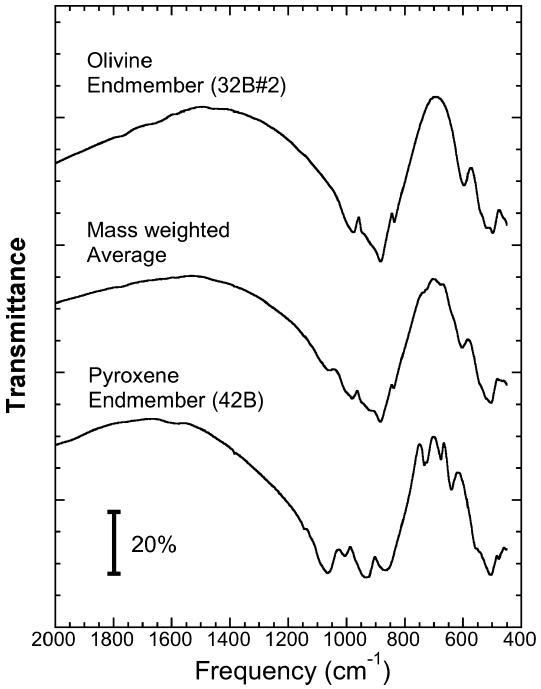

Fig. 10. The 2000–450 cm^{-1} (5.0–22.2 μm) infrared transmission spectra of the mass weighted average spectrum of all the infrared spectra taken from Almahata Sitta, except stone 25, compared to the spectra of the olivine and pyroxene spectral endmembers (32B#2 and 42B, respectively). The averaged spectrum is consistent with an olivine:pyroxene mixture of 74:26.

Thus, the olivine-to-pyroxene ratios seen in Almahata Sitta seem to be consistent with that observed in other ureilites, both in terms of the large variability from location to location within a single meteorite and in terms of the overall "bulk" ratio.

The Meteoritic Silicate Features—Mineral Chemistry

The olivines $[(X,Y)_2SiO_4]$ in ureilites are Mg-rich, typically having forsterite $[Mg_2SiO_4]$ contents ranging from Fo_{74} to Fo_{97}, with most falling between Fo_{74} and Fo_{85} (Takeda 1991; Goodrich et al. 2004; Downes et al. 2008). The exact positions of the olivine features near 985, 600, and 500 cm^{-1} vary over ranges of 20–50 cm^{-1} depending on the Mg/Fe ratio, with Mg-rich olivines 5 falling to higher frequencies (Tarte 1965; Farmer 1974). The olivine band positions summarized in Table 2 are consistent with Mg being the dominant cation in this mineral.

Interpretation of the chemistry of the pyroxenes $[(X,Y)_2Si_2O_6]$ is generally more problematic since this mineral comes in both clino and ortho forms and participates in a much wider range of cation substitutions. As a result, the silicate features produced by pyroxenes can show considerable variability. A review of the extent of this variability can be found in the extensive summary of the thermal emission spectra of pyroxene standards by Hamilton (2000). Nonetheless, it is possible to say a few things about the meteorite spectra dominated by pyroxene (Fig. 8). Comparison of the spectra of these pyroxenes with those of other ureilites (Sandford 1993), synthetic pigeonites (Estep et al. 1971), and the two pigeonite standards shown in Fig. 4 demonstrates that the profiles of these bands fall within the range of spectral variation seen within pigeonites $[(Ca,Mg,Fe)(Mg,Fe)Si_2O_6)]$. This is in agreement with pigeonite generally being the dominant pyroxene in most ureilites (Dodd 1981; Goodrich 1992; Middlefehldt et al. 1998; Goodrich et al. 2004; Downes 6 et al. 2008) and in Almahata Sitta specifically (Jenniskens et al. 2009; Zolensky et al. 2010, this issue). The spectrum of sample 15#2 differs significantly from the spectra of the other samples dominated by pyroxenes, suggesting it has a different distribution of cations. Zolensky et al. (2010, this issue) report that the pyroxenes in various stones from Almahata Sitta show a wide compositional range, so it is not surprising we see some spectral variation in the pyroxenes. Indeed, it may be surprising that more variation was not observed.

As noted earlier, sample 25 has been determined to be an H5 ordinary chondrite (Zolensky et al. 2010, this issue). This meteorite was distinct from the others examined in this study by being more mechanically robust and containing lighter colored material. Its spectrum shows the presence of nearly equal portions of olivines and pyroxenes (Fig. 9, Table 3). Other than having a somewhat higher silicate band contrast than most of the ureilite samples of this composition, there is little to distinguish the spectrum of this sample from the others examined here.

The Spectral Variability Within and Between Different Stones

A determination of "bulk" properties of the Almahata Sitta parent body requires examination of the entire ensemble of spectra. There is significant variation from sample to sample, but this variation does not correlate well with meteorite density (Shaddad et al. 2010, this issue) or albedo. As mentioned earlier, the relatively coarse grain size of ureilites (see Berkley 1986), and the visible presence of millimeter and submillimeter individual crystalline mineral grains within many of the Almahata Sitta samples suggests the strong possibility that some of our samples are sufficiently small that they fail to be representative of their original source stones as a whole. Spectra taken

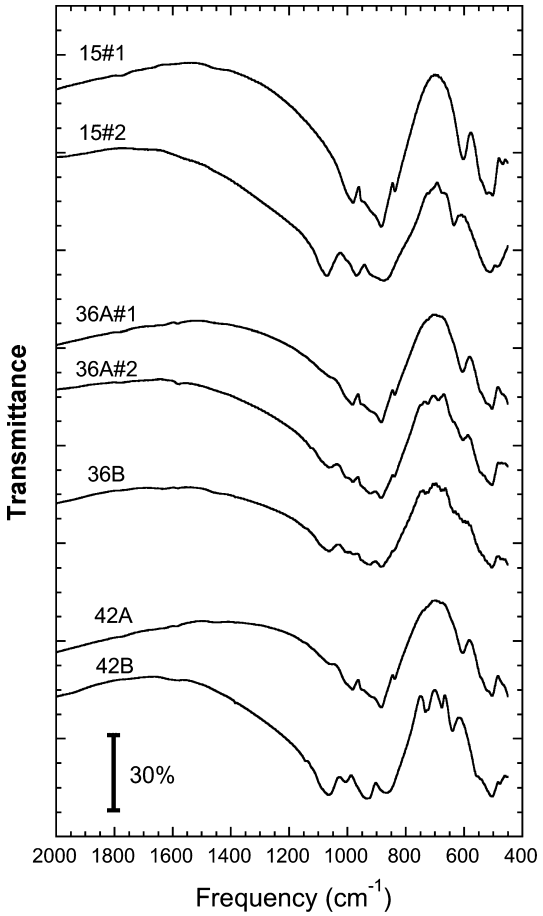

Fig. 11. The 2000–450 cm^{-1} (5.0–22.2 μm) infrared transmission spectra of seven samples taken from three stones of the Almahata Sitta meteorite. In many cases, the spectra of multiple samples from the same stone show very similar spectra, but spectra from these three stones show some of the most dramatic variations.

from multiple samples from the same stone provide some indication of the extent of this issue.

In most cases, the spectra of multiple samples from the same stone look very similar to each other. For example, see the spectra of samples 4#1, 4#2, 7B, and 7W in Fig. 5, samples 32B#1 and 32B#2 in Fig. 6, samples 39#1, 39#2, and 39#3 in Fig. 7, and samples 51#1, 51#2, 51#3, and 51#4 in Fig. 8. However, in some cases the spectra from different samples from the same stone differ significantly. Figure 11 shows three sets of spectra in which there were significant differences between the spectra of multiple samples from the same stone. Samples 15#1 and 15#2 are very dissimilar, the first being dominated by olivine and the second being dominated by a unique pyroxene that is distinctly different from all the other pyroxenes seen in this work. The differences between samples 36A#1, 36A#2, and 36B are not quite as dramatic, but still range from mixtures dominated by olivine to a mixture dominated by pyroxene (see Table 3). Finally, samples 42A and 42B again span the range from being dominated by olivine (42A) to being dominated by pyroxene (42B; which is the pyroxene spectral endmember). These data provide a clear indication that individual spectra in Figs. 5–9 cannot be assumed to be representative of all the material in their associated stones. A better determination of "bulk" properties of the Almahata Sitta meteorite requires examination of the entire ensemble of spectra (see above).

The Presence of Infrared Inactive Phases in the Samples

While all the KBr pellets have essentially the same sample concentration (1 mg sample per 100 mg KBr), the spectra shown in Figs. 5–9 show Si-O bands that have a range of band contrasts, with absolute band depth varying by substantial factors (for example, compare the spectra of samples 4#2 and 15#1 in Fig. 5). These variations are too big to be explained in terms of differences in intrinsic band strengths of the relevant minerals, particularly since the minerals in question have very similar major cation compositions. In addition, the infrared transmission continua of the spectra outside the silicate feature vary by as much as 40%, with lower continua generally associated with darker pellets. The most likely source of these differences is the presence of variable amounts of infrared-neutral material, i.e., material that can scatter and absorb infrared photons but that does not produce strong infrared features. There are a number of materials in ureilites that meet this requirement, in particular graphite, diamond, sulfides, and metals, and all of these have been identified in Almahata Sitta samples (Steele et al. 2009; Zolensky et al. 2010, this issue). Earlier investigations of sample #7 showed the presence of large concentrations of highly graphitized carbon (see Fig. 1) (Jenniskens et al. 2009; Steele et al. 2009), and this is therefore the most likely candidate for the dominant infrared-neutral material in our samples. As noted earlier, there is a general tendency for pellets to have darker colors as the olivine contribution increases, suggesting the infrared inactive material may be more closely associated with this mineral.

CONCLUSIONS

We have presented 39 mid-IR (4000–450 cm^{-1}; 2.5–22.2 μm) transmission spectra taken from 26 different stones from the Almahata Sitta meteorite, whose parent body, 2008 TC3, collided with the Earth over Sudan on October 7, 2008. The ureilite spectra show a number of absorption bands, the strongest of which is a wide,

complex feature centered near 1000 cm^{-1} (10 μm) attributed to Si-O stretching vibrations in silicates. The profile of the silicate feature varies from sample to sample and it is clear that all the spectra are dominated by mixtures containing varying proportions of olivines and pyroxenes. Mixtures span the entire range from nearly pure olivine to nearly pure pyroxene, but olivine is generally more abundant. The mass weighted average spectrum of all the ureilite samples yields an olivine:pyroxene ratio of 74:26, which falls in the middle of the range reported for other ureilites. The predominance of olivine and the variable olivine-to-pyroxene ratio (both within and between stones) are consistent with the known composition and heterogeneity of other ureilites.

The precise positions of the principle absorption bands of olivine provide a measure of the Mg/Fe ratio in the mineral. Comparison of the peak positions of the olivine bands in the Almahata Sitta spectra with those from mineral standards indicates the olivines are very Mg-rich, consistent with the known Mg-rich nature of this mineral in ureilites. The spectra dominated by pyroxene are consistent with an assignment to pigeonite, in agreement with the mineralogy of many ureilites and Almahata Sitta stone #7. One unique sample, 15#2, yielded a pyroxene-dominated spectrum distinctly different from the other pyroxenes, suggesting it had a distinctly different cation distribution.

Variations in the intrinsic strength of the silicate feature and its surrounding infrared continuum indicate the variable presence of material with no strong infrared absorption bands. The most likely candidate for this infrared-neutral material is graphitized carbon, but diamond and metals could contribute. Darker samples, presumably richer in carbon, tend to have higher olivine/pyroxene ratios.

Acknowledgments—We thank the many students and staff of the University of Khartoum for their support in helping recover the meteorites. We also thank Dr. Michael Zolensky for providing the images of Almahata Sitta #7. The authors are grateful for helpful comments from H. Downes, M. Gaffey, and an anonymous reviewer that resulted in improvements to this manuscript. The authors are also grateful for support from the NASA Origins of Solar Systems Program (grant 811073.02.07.02.54) and the NASA Planetary Astronomy Program. The pigeonite standards used in this paper were kindly provided by the American Museum of Natural History, Smithsonian Institution, Department of Mineral Sciences.

Editorial Handling—Dr. Michael Gaffey

REFERENCES

Berkley J. L. 1986. Four Antarctic ureilites: Petrology and observations on ureilite petrogenesis. *Meteoritics* 21:169–189.

Berkley J. L., Brown H. G., IV, Keil K., Carter N. L., Mercie J.-C. C., and Huss G. 1976. The Kenna ureilite: An ultramafic rock with evidence for igneous, metamorphic, and shock origin. *Geochimica et Cosmochimica Acta* 40:1429–1437.

Berkley J. L., Taylor G. J., and Keil K. 1978. Fluorescent accessory phases in the carbonaceous matrix of ureilites. *Geophysical Research Letters* 5:1075–1078.

Berkley J. L., Taylor G. J., Keil K., Harlow G. E., and Prinz M. 1980. The nature and origin of ureilites. *Geochimica et Cosmochimica Acta* 44:1579–1597.

Bischoff A., Scott E. R. D., Metzler K., and Goodrich C. A. (2006). Nature and origin of meteoritic breccias. In *Meteorites and the early solar system II*, edited by Lauretta D. S. and McSween H. Y. Jr. Tucson, AZ: The University of Arizona Press. pp. 679–712.

Bischoff A., Horstmann M., Laubenstein M., and Haberer S. 2010. Asteroid 2008 TC3—Almahata Sitta: Not only a ureilitic meteorite, but a breccia containing many different achondritic and chondritic lithologies (abstract #1763). 41st Lunar and Planetary Science Conference. CD-ROM.

Borovicka J. and Charvat Z.. 2009. Meteosat observation of the atmospheric entry of 2008 TC3 over Sudan and the associated dust cloud. *Astronomy & Astrophysics*, in press. 7

Brown P. G. 2008. *US Government Release: Bolide Detection Notification 2008–282*. http://aquarid.physics.uwo.ca/~pbrown/usaf/usg282.txt. Accessed October 15, 2008.

Chesley S., Chodas P., and Yeomans S. 2008. *NASA/JPL Near-Earth Object Program Office Statement*. http://neo.jpl.nasa.gov/news/2008tc3.html. Accessed November 4, 2008.

Dodd R. T. 1981. *Meteorites: A petrologic-chemical synthesis*. Cambridge, UK: Cambridge University Press. pp. 293–304.

Downes H., Mittlefehldt D. W., Kita N. T., and Valley J. W. 2008. Evidence from polymict ureilite meteorites for a disrupted and re-accreted single ureilite parent asteroid gardened by several distinct impactors. *Geochimica et Cosmochimica Acta* 72:4825–4844.

Estep P. A., Kovach J. J., and Karr Jr. C. 1971. Infrared vibrational spectroscopic studies of minerals from Apollo 11 and Apollo 12 lunar samples. Proceedings, 2nd Lunar Science Conference. pp. 2137–2151.

Farmer V. C. 1974. Orthosilicates, pyrosilicates, and other finite-chain silicates. In *The infrared spectra of minerals*, edited by Farmer V. C. Mineralogical Society Monograph 4, London: Mineralogical Society. pp. 285–303.

Gaffey M. J., Burbine T. H., Piatek J. L., Reed K. L., Chaky D. A., Bell J. F., and Brown R. H. 1993. Mineralogic variations within the S-type asteroid class. *Icarus* 106:573–602.

Goodrich C. A. 1992. Ureilites: A critical review. *Meteoritics* 27:327–352.

Goodrich C. A., Scott E. R. D., and Fioretti A. M. 2004. Ureilitic breccias: Clues to the petrologic structure and impact disruption of the ureilite parent asteroid. *Chemie der Erde – Geochemistry* 64:283–327.

Hamilton V. E. 2000. Thermal infrared emission spectroscopy of the pyroxene mineral series. *Journal of Geophysical Research* 105:9701–9716.

Horstmann M. and Bischoff A. 2010. Characterization of spectacular lithologies from the Almahata Sitta breccia (abstract #1784). 41st Lunar and Planetary Science Conference. CD-ROM.

Jenniskens P., Shaddad M. H., Numan D., Elsir S., Kudoda A. M., Zolensky M. E., Le L., Robinson G. A., Friedrich J. M., Rumble D., Steele A., Chesley S. R., Fitzsimmons A., Duddy S., Hsieh H. H., Ramsay G., Brown P. G., Edwards W. N., Tagliaferri E., Boslough M. B., Spalding R. E., Dantowitz R., Kozubal M., Pravec P., Borovicka J., Charvat Z., Vaubaillon J., Kuiper J., Albers J., Bishop J. L., Mancinelli R. L., Sandford S. A., Milam S. N., Nuevo M., and Worden S. P. 2009. The impact and recovery of asteroid 2008 TC_3. *Nature* 458:485–488.

Kowalski R. A. et al. 2008. In *MPEC 2008–T50*, edited by Williams G. V. 1–1: Minor Planet Center, Smithsonian Astrophysical Observatory.

Middlefehldt D. W., McCoy T. J., Goodrich C. A., and Kracher A. 1998. Non-chondritic meteorites from asteroidal bodies. In *Planetary materials*, edited by Papike J. J., Reviews I Mineralogy 36:4-1 to 4-195.

Miyamoto M. 1987. Infrared diffuse reflectances (2.5–25 μm) of some meteorites. *Icarus* 70:146–152.

Salisbury J. W., D'Aria D. M., and Jarosewich E. 1991. Mid-infrared (2.5–13.5 μm) reflectance spectra of powdered stony meteorites. *Icarus* 92:280–297.

Sandford S. A. 1984. Infrared transmission spectra from 2.5 to 25 μm of various meteorite classes. *Icarus* 60:115–126.

Sandford S. A. 1993. The mid-infrared transmission spectra of Antarctic ureilites. *Meteoritics* 28:579–585.

Shaddad M., Jenniskens P., Kudoda A., Numan D., Elsir S., Riyad I., Ali A., Alameen M., Alameen N., Eid O., Osman A., AbuBaker M., Chesley S., Chodas P., Albers J., Edwards W., Brown P., Kuiper J., and Friedrich J. 2010. The recovery of asteroid 2008 TC_3. *Meteoritics & Planetary Science* 45. This issue.

Steele A., Fries M., Jenniskens P., and Zolensky M. 2009. Characterisation of diamond in the Almahata Sitta meteorite (abstract 9.08). *DPS-AAAS*.

Takeda H. 1987. Mineralogy of Antarctic ureilites and a working hypothesis for their origin and evolution. *Earth and Planetary Science Letters* 81:358–370.

Takeda H. 1991. Comparisons of Antarctic and non-Antarctic achondrites and possible origin of the differences. *Geochimica et Cosmochimica Acta* 55:35–47.

Takeda H., Mori H., and Ogata H. 1989. Mineralogy of augite-bearing ureilites and the origin of their chemical trends. *Meteoritics* 24:73–81.

Tarte P. 1965. Experimental study and interpretation of infrared spectra of silicates and germanates. *Mem. R. Belg. Cl. Sci.* 8° 35: parts 4a,b.

Tholen D. J. 1984. Asteroid taxonomy from cluster analysis of photometry. Ph.D. thesis, The University of Arizona Press.

Tholen D. J. 1989. In *Asteroids II*, edited by Matthews M. S., Binzel R. P., and Gehrels T. The University of Arizona Press. pp. 1139–1150.

Vdovykin G. P. 1970. Ureilites. *Space Science Reviews* 10:483–510.

Yeomans D. 2008. *NASA/JPL Near-Earth Object Program Office Statement*. http://neo.jpl.nasa.gov/news/news159.html. Accessed October 6, 2008.

Zolensky M. E., Herrin J., Mikouchi T., Ohsumi K., Friedrich J. M., Steele A., Fries M., Sandford S. A., Milam S., Hagiya K., Takeda H., Satake W., Kurihara T., Colbert M., Hanna R., Maisano J., Ketcham R., Le L., Robinson G. A., Martinez J. E., Jenniskens P., and Shaddad M. H. 2010. Mineralogy and petrography of the Almahata Sitta ureilite. *Meteoritics & Planetary Science* 45. This issue.

Author Query Form

Journal: MAPS

Article: 1096-1257

Dear Author,
During the copy-editing of your paper, the following queries arose. Please respond to these by marking up your proofs with the necessary changes/additions. Please write your answers on the query sheet if there is insufficient space on the page proofs. Please write clearly and follow the conventions shown on the attached corrections sheet. If returning the proof by fax do not write too close to the paper's edge. Please remember that illegible mark-ups may delay publication.

Many thanks for your assistance.

Query reference	Query	Remarks
1	**AUTHOR: Goodrich (2004) has been changed to Goodrich et al. (2004) so that this citation matches the Reference List. Please confirm that this is correct.**	
2	**AUTHOR: Mittlefehldt et al. (1998) has been changed to Middlefehldt et al. (1998) so that this citation matches the Reference List. Please confirm that this is correct.**	
3	**AUTHOR: Hostmann and Bischoff (2010) has been changed to Horstmann and Bischoff (2010) so that this citation matches the Reference List. Please confirm that this is correct.**	
4	**AUTHOR: Please give address information for 'Sigma-Aldrich': city, state (if applicable), and country.**	
5	**AUTHOR: falling to—Please check if this should read *falling at*?**	
6	**AUTHOR: Goodrich 2004 has been changed to Goodrich et al. 2004 so that this citation matches the Reference List. Please confirm that this is correct.**	
7	**AUTHOR: Please provide the volume number, page range for reference Borovicka, and Charvat (2009).**	
8	**AUTHOR: Please provide the document title, city location of publisher, page range for reference Kowalski, et al. (2008).**	
9	**AUTHOR: Journal style is to include all author names for each reference in the reference list. Please replace all appearances of 'et al.' in your reference list with the complete author lists.**	
10	**AUTHOR: Please provide the name of the publisher, city location of publisher for reference Middlefehldt et al. (1998).**	
11	**AUTHOR: Please provide more details for reference 'Steele et al. 2009'.**	
12	**AUTHOR: Please provide full form for journal title 'Mem. R. Belg. Cl. Sci' for reference Tarte (1965).**	

13	**AUTHOR: Tholen (1984) has not been cited in the text. Please indicate where it should be cited; or delete from the Reference List.**	
14	**AUTHOR: Please provide city, state and country for reference Tholen 1984.**	
15	**AUTHOR: Please provide the document title, city location of publisher for reference Tholen (1989).**	

Proof Correction Marks

Please correct and return your proofs using the proof correction marks below. For a more detailed look at using these marks please reference the most recent edition of The Chicago Manual of Style and visit them on the Web at: http://www.chicagomanualofstyle.org/home.html

Instruction to typesetter	*Textual mark*	*Marginal mark*
Leave unchanged	under matter to remain	stet
Insert in text the matter indicated in the margin	∧	∧ followed by new matter
Delete	through single character, rule or underline or through all characters to be deleted	
Substitute character or substitute part of one or more word(s)	through letter or through characters	new character or new characters
Change to italics	under matter to be changed	ital
Change to capitals	under matter to be changed	caps
Change to small capitals	under matter to be changed	sc
Change to bold type	under matter to be changed	bf
Change to bold italic	under matter to be changed	bf+ital
Change to lower case		lc
Insert superscript	∨	∨ under character e.g. ∨
Insert subscript	∧	∧ over character e.g. ∧
Insert full stop	⊙	⊙
Insert comma		
Insert single quotation marks		
Insert double quotation marks		
Insert hyphen		
Start new paragraph		
Transpose		
Close up	linking characters	
Insert or substitute space between characters or words	#	#
Reduce space between characters or words		